

周向弯曲方向对 NACA65 翼型轴流叶轮叶顶间隙流动影响

颜培弟,金光远,崔政伟

(江南大学 机械工程学院 江苏 无锡 214122)

摘要: 本研究采用三维气动设计方法设计了具有 NACA65-810 翼型的直叶轮、周向前弯和周向后弯叶轮,并采用计算流体力学软件模拟其气动性能,分析了压力峰值工况和设计工况下 3 个叶轮叶顶泄漏流和泄漏涡的空间发展和叶顶间隙部分静压损失以及熵分布。结果表明:直叶轮引入周向前弯后,叶顶泄漏流的卷吸能力降低,泄漏涡起源位置向远离叶片前缘的方向迁移,泄漏涡涡心径向高度得到了保持,降低了叶顶泄漏流与主流的干涉作用;引入周向后弯后,泄漏流的卷吸能力增强,泄漏涡的起源位置向靠近叶片前缘的方向迁移,远离叶片前缘的涡心径向高度显著降低,涡核下游弥散范围扩大,增强了叶顶泄漏流与主流的干涉作用,不利于降低叶顶泄漏损失。

关键词: NACA65 翼型;周向弯曲;叶顶间隙;泄漏流;数值分析

中图分类号:TH312 文献标识码:A

DOI:10.16146/j.cnki.rndlge.2016.11.004

引言

叶顶泄漏流动对叶轮机械的气动性能具有重要影响,其造成的流动损失影响范围可以达到 30% 叶高,甚至严重影响叶轮机械的稳定运行范围。弯掠技术提出和应用以后,其在提高效率、降低噪声和扩大稳定工作范围上的表现促使更多学者对其进行研究。近年来,已有部分弯掠技术对叶顶泄漏流动影响的相关研究,国外学者 T. Wantanabe 等人采用 N-S 方程计算了透平叶栅的叶顶间隙泄漏流动^[1]; J. B. Staubach 对叶片弯、掠等形式对叶顶间隙流动的影响进行了数值分析^[2], GONG 等人对一前掠轴流风扇峰值效率工况下叶顶泄漏流动结构进行了数值和试验分析^[3],结果发现叶顶泄漏流的卷吸起源

于最大静压差部分并沿压力中心线向下游发展,叶顶和端壁间的反向流动是由叶顶泄漏流的阻滞作用造成。国内学者贾希诚等人用数值方法研究了不同壁面边界条件和不同叶顶间隙下泄漏流与通道二次流的相互作用机理^[4]。李杨等人分析了低压轴流风扇叶片不同周向前弯角度对叶顶泄漏流的影响^[5-6],总结出叶顶泄漏流的轴向位移随周向弯曲角度的增加呈现先减小后增加的变化,周向位移变化则相反;金光远等人研究了圆弧板翼型周向弯曲叶片叶顶泄漏流及涡核的变化规律^[7-8];陈金鑫等人模拟了某微型轴流风机不同流量下的三维流场^[9],指出了叶顶分离涡及泄漏流的起因以及泄漏流速和流量的影响因素;刘洋等人采用 Realizable $k-\varepsilon$ 湍流模型和 Simple 算法模拟了某轴流通风机^[10],分析了不同叶顶间隙对风机性能的影响。然而,由于目前轴流风机叶片翼型多种多样,弯掠的组合方式也不尽相同,弯掠对叶顶泄漏流动的影响还没有定论,仍需进一步的研究。本文采用研究较少的 NACA65-810 翼型设计具有直叶片、周向前弯和周向后弯叶片的轴流叶轮并进行数值模拟,分析周向弯曲方向对具有这一翼型的轴流叶轮叶顶泄漏流的影响,以为后续的研究应用提供借鉴。

1 NACA 翼型简介

NACA 翼型由美国航空航天局开发,翼型代号由“NACA”和一连串数值组成,数值描述翼型的设计按所带数值可分为 4~8 位数型以及以上系列的修改型,不同的系列具有不同的设计参数。其中的 4 位数和 5 位数系列中的基础翼型目前在国内的研究

收稿日期:2015-07-28; 修订日期:2015-09-11

基金项目:江苏省自然科学基金青年基金项目(BK20130150)

作者简介:颜培弟(1988-),男,河南平顶山人,江南大学工学硕士。

和应用较多 6 位数则研究应用较少,本文采用这一系列中的 810 翼型设计轴流叶轮(设计参数参考文献[11~13])并分析其叶顶泄漏流动情况,以期分析这一系列翼型的轴流叶轮叶顶泄漏流动特点,为后续研究提供借鉴。

2 数值模型及计算方法

采用 NACA65-810 翼型设计具有直叶片、周向前弯和周向后弯特征叶片的轴流叶轮,叶片采用孤立翼型设计方法和变环量流型分配径向载荷。叶轮设计参数为:设计流量 $3 \text{ m}^3/\text{s}$,设计全压 140 Pa ,转速 1450 r/min ,轮毂比 0.35 ,叶顶间隙 3 mm ,叶片数为 5 ,截面积叠方式为重心积叠,周向弯曲叶片的积叠线由直线段引入周向弯曲形成,周向弯曲角度取研究较多的 8.3° ,积叠线由交点位于 0.4 相对叶高的直线段和圆弧组成,两者分别位于叶根和叶顶,积叠线和 3 叶轮模型如图 1 所示。为叙述方便,以下分别简称直叶轮、前弯叶轮和后弯叶轮。

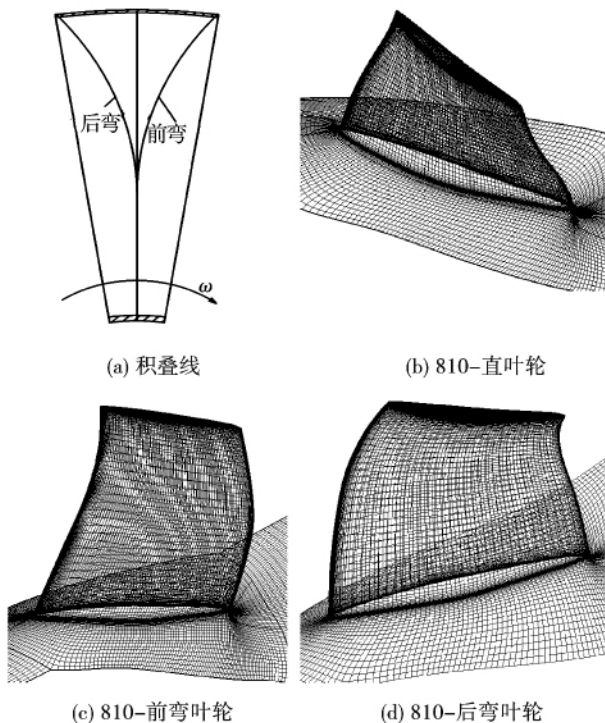


图 1 积叠线及叶轮模型

Fig. 1 Stacking lines and model for impellers

分别采用 Numeca/IGG 和 Numeca/Fine™ 对叶轮单通道流场进行网格划分和计算求解,数值模型采用 S-A 湍流模型,并采用四阶龙格-库塔法对

计算进行时间推进,壁面第一层网格的 y^+ 值控制在 1 附近,对壁角处网格采用加密的处理方式提高计算精度,网格总量约 75 万,网格分布为:流向 \times 转向 \times 展向 $= 139 \times 65 \times 73$,叶片周围 O 型网格分布为: 193×73 ,叶顶间隙网格分布为: $193 \times 17 \times 17$ 。网格无关性分析分别取 55 万和 100 万,计算结果对比发现 75 万网格计算结果与 100 万网格计算结果相近且 75 万网格计算耗时更少。设计工况边界条件给定进口总压 101506.8 Pa 、总温 293 K 和出口流量 3.63 kg/s ,压力峰值工况进口边界条件与设计工况相同,出口给定流量 3.267 kg/s ,叶轮进出口给定周期性边界条件,壁面给定绝热无滑移条件,收敛残差给定 $1e-6$ 。

3 计算结果及分析

3.1 泄漏流空间发展

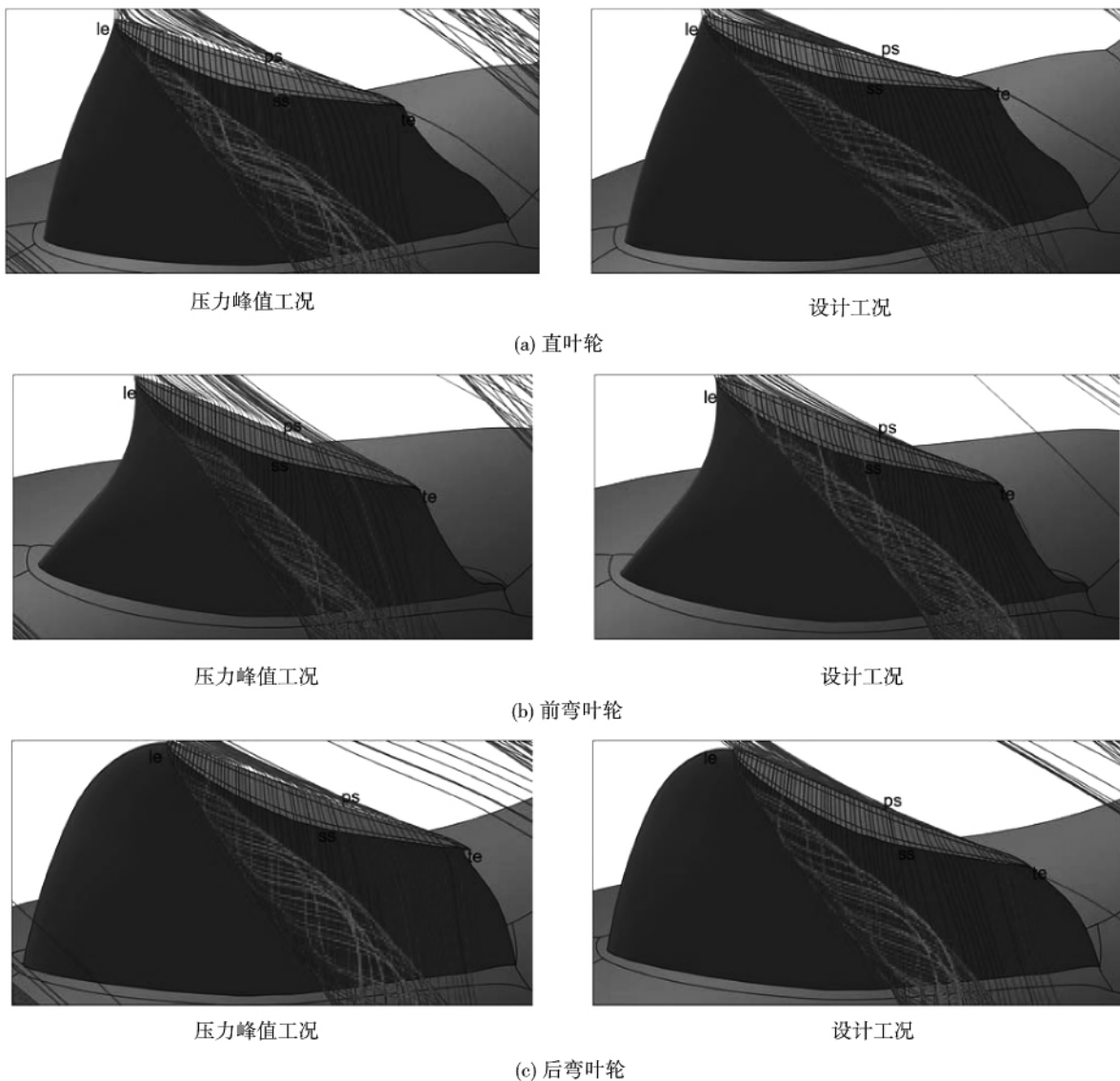
图 2 为压力峰值工况(流量系数 $\phi = 0.44$,全压系数 $\psi = 0.13$)和设计工况(流量系数 $\phi = 0.49$,全压系数 $\psi = 0.11$)下 3 个叶轮叶顶间隙部分的相对速度流线图,叶顶泄漏流起源于叶顶叶尖,向下游发展过程中涡核弥散加剧并逐渐衰灭。由图 2 可以看出,直叶轮由设计工况进入压力峰值工况后,叶顶泄漏起始位置向叶顶前缘迁移,下游涡的弥散范围扩大;周向前弯叶轮具有同样的变化并且涡核弥散范围扩大尤为明显,泄漏流的起始位置相比直叶轮向远离叶顶前缘的位置迁移,同一工况下周向前弯叶轮叶顶泄漏流下游的弥散程度明显低于直叶轮;后弯叶轮涡核弥散范围则明显扩大,泄漏流起始位置明显向靠近叶顶前缘的位置迁移,其卷吸作用也明显高于直叶轮。在压力峰值工况下,直叶轮的泄漏流卷吸能力最强,后弯叶轮的涡核弥散范围最大,设计工况下周向后弯叶轮泄漏流起始位置最靠近叶顶前缘,不利于降低叶顶泄漏流的影响。

3.2 泄漏流涡心位置变化

为分析 3 个叶轮泄漏流涡心偏离设计流量时的变化及周向弯曲对叶顶泄漏流涡心位置的影响,将叶顶沿周向划分为 7 个部分,以 8 个截面内相对速度等值线的低速核心表示截面内泄漏流涡心位置。图 3 所示为叶顶划分示意图和两种工况下泄漏流涡核的变化。由图 3(b)可以看出,直叶轮由设计流量进入压力峰值流量后同一截面内泄漏流涡心位置明显降低,两种工况下涡心在整个弦长范围内呈现出

同步变化;直叶轮引入周向前弯后两种工况下涡心位置具有与直叶轮相同的变化规律,不同的前弯叶轮涡心径向位置先上升后降低,在 0.7 弦长以后涡心径向位置逐渐趋于一致;直叶轮引入周向后弯后涡心径向位置在两种工况下具有同步变化,涡心径向位置下降速率也明显高于直叶轮。直叶轮引入周向后弯后,同一工况下截面径向位置显著降低,引入周向前弯后在 0.55 弦长以内涡心位置具有明显降低,0.55 弦长以后范围内直叶轮的涡心位置则低于前弯叶轮。而从两种工况下同一截面(图 3(c))内涡核的弥散可以看出,由设计工况进入压力峰值工况后涡核的弥散范围扩大,由等值线值可看出,涡的

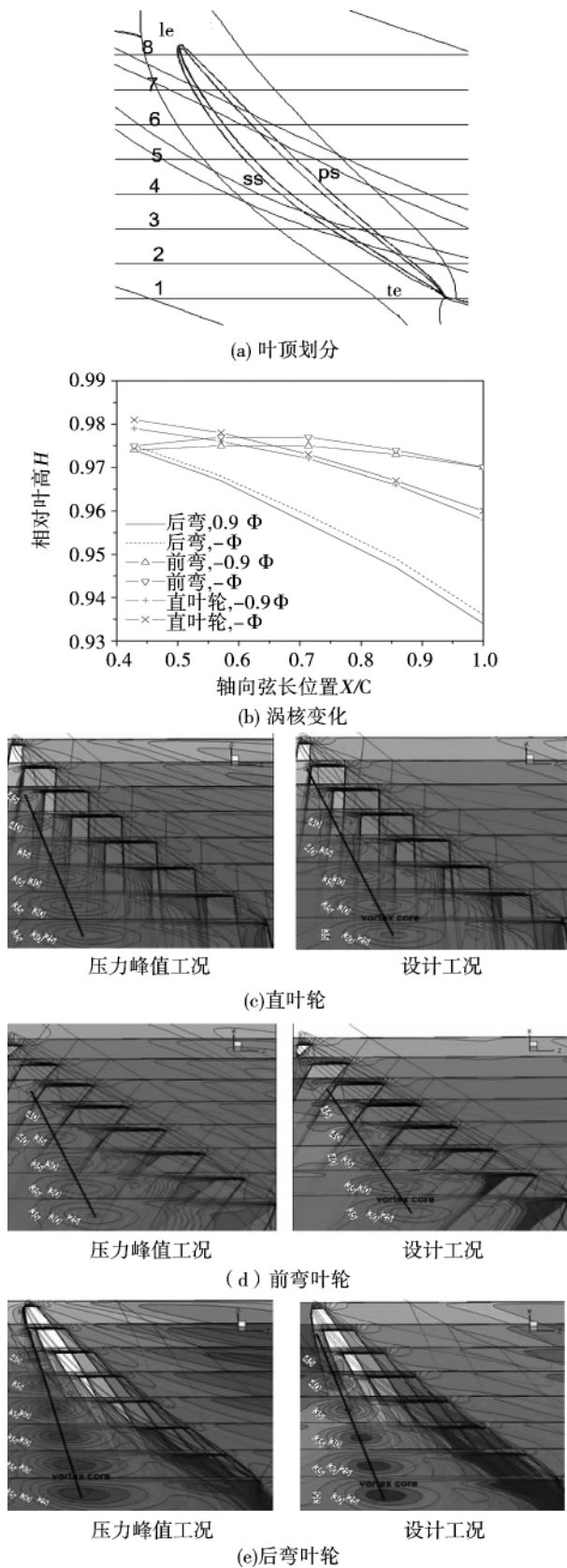
卷吸作用明显增加;直叶轮引入周向前弯后涡核弥散程度有小幅降低,涡的起源由距叶顶前缘 0.14 弦长(第 7 截面)增加到 0.29 弦长(第 6 截面),而引入后弯后涡核弥散范围则明显扩大,涡核起源则没有明显变化,泄漏涡的卷吸作用则明显增强。由此可以看出,直叶轮引入周向前弯后,叶顶泄漏涡的涡心径向位置得到了保持,降低了叶顶泄漏涡与主流的干涉作用,涡核弥散程度有显著降低,涡核起源向下游移动;引入周向后弯后涡心径向高度降低,叶顶泄漏涡与通道内的主流干涉作用增强,涡卷吸作用明显增强,不利于降低叶顶泄漏流的影响。



注:ps - 压力面;ss - 吸力面;le - 前缘;te - 尾缘

图 2 叶顶泄漏流变化

Fig 2 Changes of the blade tip leakage flow



注:0.9Φ—压力峰值工况,Φ—设计工况。

图3 叶顶划分及涡核变化

Fig.3 Blade tip division and changes of the vortex cores

3.3 变工况上端壁极限流线变化

图4为3个叶轮压力峰值工况和设计工况下的上端壁极限流线。由图可以看出,3个叶轮的流线都在吸力面一侧(SS)汇聚成一条分离线(SL),而从分离线起始点距前缘的距离可以看出,直叶轮引入周向前弯后分离线起始点向下游移动,引入周向后弯后起始点则明显向前缘移动;由设计工况进入压力峰值工况后,直叶轮和前弯叶轮的分离线起始点没有明显变化,而后弯叶轮的起始点则明显迁移到叶顶叶尖,以上变化和泄漏涡的变化规律相同,验证了周向前弯和后弯对叶顶泄漏涡的影响规律。

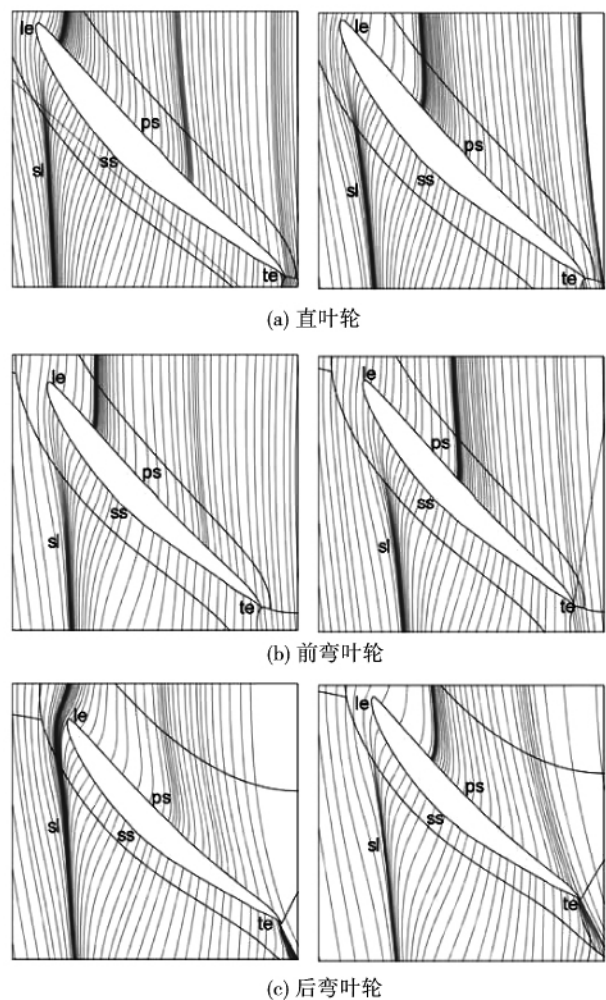


图4 上端壁极限流线

Fig.4 Streamlines on the top end wall

为考察叶顶泄漏涡的强度,分析子午面内叶顶间隙部分的能量损失分布,如图5所示。相对总压损失系数CP定义为^[14]:

$$CP \times 1 = \frac{P_{t_{inlet}} - P_t}{P_{t_{inlet}}} \quad (1)$$

式中: $p_{t_{inlet}}$ —进口总压, Pa; p_t —当地总压, Pa;

直叶轮由设计工况进入压力峰值工况后总压高损失区域明显扩大,最高损失区域由叶顶尾缘向叶中部分移动,而尾缘径向损失范围的扩大尤为明显;前弯叶轮最高损失区域也有所扩大,径向损失增加趋势与直叶轮相同,但高损失区域仍保持在叶顶尾缘;后弯叶轮由设计工况进入压力峰值工况后损失范围和损失数值都明显增加,高损失区域也由叶顶

弦长中部向叶顶前缘移动。在压力峰值工况下,直叶轮叶顶高损失区域和损失值都最小,后弯叶轮无论损失区域还是损失量都最高;设计工况下,周向弯曲叶轮具有同样的表现。以上分析表明,周向后弯增加了叶顶泄漏涡的强度和影响范围,周向前弯则具有减小叶顶泄漏涡的强度和影响范围的作用。这与周向前弯抑制了气流的径向流动,减小了径向气流流动对端壁的冲击作用,改善端壁附近的流动情况相一致。以上分析结果与泄漏涡涡心位置空间变化和端壁极限流线分析结果相一致。

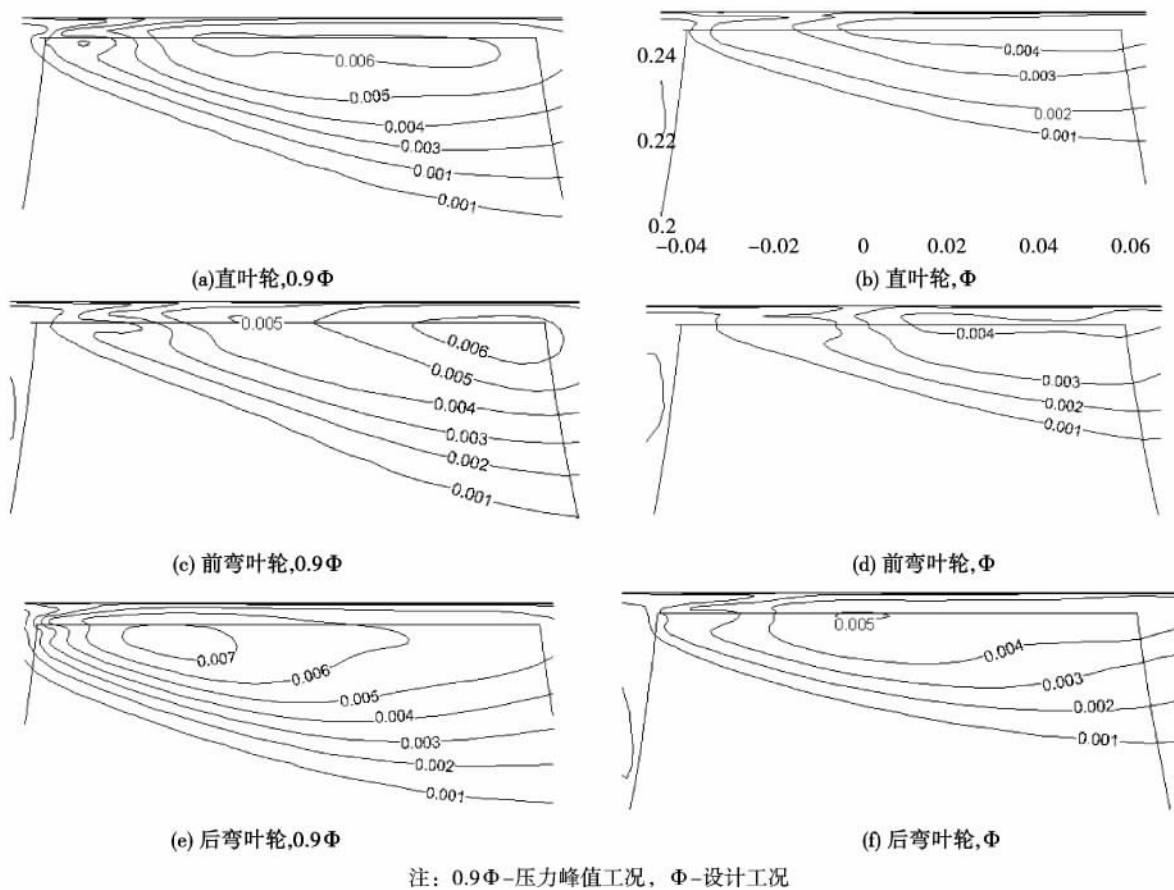


图 5 叶顶间隙相对总压损失系数分布

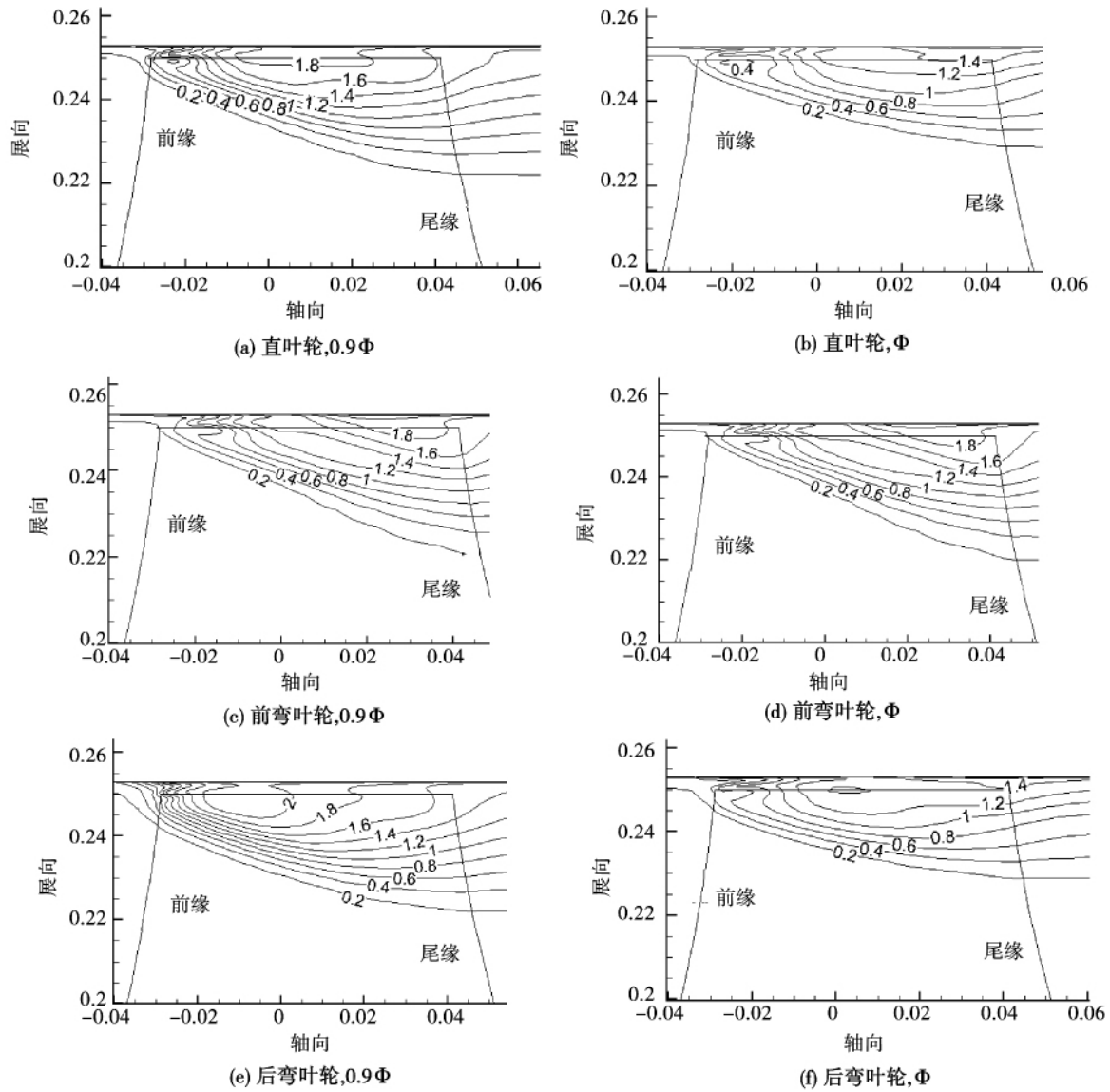
Fig 5 Distribution of the static pressure coefficient in the blade tip clearance

图 6 为 3 个叶轮两种工况下子午面内叶顶间隙部分的熵分布。由图中可以看出,在压力峰值工况下直叶轮的最大损失区域位于叶顶中间部分,与总压最高损失区域相一致,引入周向前弯后最高损失

区域向尾缘移动,引入周向后弯后损失区域向叶顶前缘移动,并且损失值和范围都有明显增加;在设计工况下直叶轮引入周向前弯后尾缘最大损失值增加较为明显,尾缘损失值 0.2 范围也由 0.23 叶高发展

到 0.22 叶高, 引入周向后弯后损失值和区域则没有明显变化。而从两种工况下的最高损失区域分布来看, 熵分布与相对总压损失分布高度一致。同时也

表明 3 种叶轮在设计工况下比在压力峰值工况下具有较高的能量转换能力。



注: 0.9Φ-压力峰值工况, Φ-设计工况

图 6 子午面熵分布

Fig. 6 Distribution of the entropy on the meridional plane

4 结 论

本文考察了具有 NACA65-810 翼型的直叶轮、周向前弯和周向后弯叶轮在压力峰值工况和设计工况下的叶顶泄漏流和泄漏流的空间发展情况以及总

压损失和熵分布, 结果表明:

- (1) 直叶轮引入周向前弯后, 在同一工况下叶顶泄漏流的卷吸能力降低, 泄漏涡起源位置向叶片尾缘移动, 泄漏涡涡心径向高度得到了保持, 降低了泄漏涡与主流的干涉作用。
- (2) 直叶轮引入周向后弯后, 在同一工况下叶

顶泄漏涡的卷吸作用增强,泄漏涡的起源位置向叶片前缘移动,远离叶顶前缘部分的涡心径向高度降低,下游弥散程度增加,加剧了叶顶泄漏流与主流的干涉作用。

(3) 从周向前弯叶轮、直叶轮和周向后弯叶轮同一工况下叶顶泄漏涡起源位置的变化可以推测在 -8.3° (向与转向相反方向弯曲) 到 $+8.3^\circ$ (向与转向相同方向弯曲) 周向弯曲角度范围内,随着弯角的增加,叶顶泄漏涡的起源位置向叶顶尾缘移动。

(4) 比较同一工况下叶顶泄漏涡的强度和影响范围可以明显看出,周向前弯可以弱化叶顶泄漏涡的影响,降低叶顶泄漏损失,周向后弯作用则正相反。

(5) 对比设计工况和压力峰值工况下的相对总压损失和熵分布可知设计工况下叶轮具有较高的能量转换效率。

参考文献:

- [1] Wantanabe T, Nozaki O, Kikuehi K, et al. Numerical simulation of the flow through cascade with tip clearance [R]. ASME FED-120, Numerical Simulations in Turbomachinery, 1991.
- [2] Staubach J B, Sharma O P, Stetson G. M. Reduction of tip clearance losses through 3-D airfoil designs [R]. Proc. R. ASME96 - TA - 13 Conference, Singapore, 1991.
- [3] Gong Hee LEE, Je Hyun BAEK, Hwan Joo MYUNG. Structure of tip leakage flow in a forward-swept axial-flow fan [J]. Flow, Turbulence and Combustion, 2003, 70: 241 - 265.
- [4] 贾希诚, 王正明, 王嘉伟. 叶轮机械中的泄漏流与泄漏涡 [J]. 工程热物理学报, 2003 (5): 753 - 756.
JIA Xi-cheng, WANG Zheng-ming, WANG Jia-wei. Leakage flow and vortexes in turbomachinery [J]. Journal of Engineering Thermophysics, 2003 (5): 753 - 756.
- [5] 李杨, 卢纪富. 叶片的周向前弯角度对低压轴流风扇叶顶泄漏流场的影响 [J]. 热能动力工程, 2009 (3): 286 - 290, 406 - 407.
LI Yang, LU Ji-fu. Influence of the circumferentially forward skew angle of blades on the blade tip leakage flow field of a low-pressure axial flow fan [J]. Engineering for Thermal Energy and Power, 2009 (3): 286 - 290, 406 - 407.
- [6] 李杨, 欧阳华, 杜朝辉. 周向弯曲低压轴流风机叶顶泄漏流动数值研究 [J]. 工程热物理学报, 2005 (2): 240 - 242.
LI Yang, OUYANG Hua, DU Chao-hui. Numerical study of the blade tip leakage flow of a circumferentially skewed low pressure axial flow fan [J]. Journal of Engineering Thermophysics, 2005 (2): 240 - 242.
- [7] 金光远, 欧阳华, 杜朝辉. 周向弯曲叶片叶顶泄漏流随流量变化特性数值研究 [J]. 航空动力学报, 2009 (9): 2107 - 2114.
JIN Guang-yuan, OUYANG Hua, DU Chao-hui. Numerical study of the characteristics governing the changes of the blade tip leakage flow of a circumferentially bent blade with the flow rate [J]. Journal of Aerospace Power, 2009 (9): 2107 - 2114.
- [8] 金光远, 吴亚东, 欧阳华, 等. 小流量下周向弯曲叶片叶顶泄漏流特性的实验研究 [J]. 空气动力学学报, 2013 (2): 198 - 203.
JIN Guang-yuan, WU Ya-dong, OUYANG Hua, et al. Experimental study of the blade tip leakage flow characteristics of a circumferentially bent blade at a small flow rate [J]. Journal of Aerospace Power, 2013 (2): 198 - 203.
- [9] 陈金鑫, 赖焕新. 微型轴流风扇间隙流动分析 [J]. 华东理工大学学报 (自然科学版), 2013 (3): 356 - 363.
CHEN Jin-xin, LAI Huan-xin. Analysis of the flow in the clearances of a miniature axial flow fan [J]. Journal of East China University of Science and Technology (Natural Science Edition), 2013 (3): 356 - 363.
- [10] 刘洋, 杨志刚. 叶顶间隙对轴流风机内部流场影响的研究 [J]. 风机技术, 2013 (2): 9 - 14.
LIU Yang, YANG Zhi-gang. Study of the influence of the blade tip clearance on the internal flow field inside an axial flow fan [J]. Fan Technology, 2013 (2): 9 - 14.
- [11] Bogdonoff, S. M.; NACA Cascade Data for the Blade Design of High Performance Axial Flow Compressors [J]. Journal of the Aeronautical Sciences, 1971, 15 (2): 89 - 95.
- [12] Herrig, L. Joseph, Ehery, J. smc. Systematic two-dimensional cascade tests of NACA 65-series compressor blades at low speeds [R]. NACA TN 3916, 1957. (Supersedes NACA RM L51G31.)
- [13] Felix, A. R.; Summary of 65-Series Compressor Blade Low Speed Cascade Data by Use of The Carpet Plotting Technique [J]. National Advisory Committee for Aeronautics Collection, 1957.
- [14] 喻雷, 常海萍. 涡轮叶冠间隙流动特性实验 [J]. 航空动力学报, 2011 (12): 2772 - 2776.
YU Lei, CHANG Hai-ping. Experiment of tip leakage flow characteristics in turbine shroud [J]. Journal of Aerospace Power, 2011 (12): 2772 - 2776.

(刘瑶 编辑)

at the air side under the wet operating condition as well as the heat transfer coefficient at the air side will all decrease with a decline of the ambient pressure, however, the amount of latent heat exchanged in unit mass will be kept almost unchanged and the proportion of the amount of latent heat exchanged will somewhat increase. At a same ambient pressure, the relative humidity of the air at the inlet will have no big influence on the amount of sensible heat exchanged in the heat exchanger but notable influence on the amount of latent heat exchanged. When the relative humidity is 40%, 60% and 80% respectively, the difference among the amounts of sensible heat exchanged will be less than 5% and when the relative humidity is 80%, the amount of latent heat exchanged will be 5.9 to 6.8 times higher than that when the relative humidity is 40%. **Key words:** wet operating condition, low atmospheric pressure, relative humidity, latent heat exchange

石墨纳米溶液的沸腾传热特性研究 = **Study of the Boiling Heat Transfer Characteristics of a Graphite Nano Solution** [刊 汉]/LI Hu-ang, MEI Yong, ZHANG Bo-tao, GONG Sheng-jie (College of Mechanical and Power Engineering, Shanghai Jiaotong University, Shanghai, China, Post Code: 200240) // Journal of Engineering for Thermal Energy & Power. - 2016, 31(11). - 14 ~ 18

To investigate the enhanced boiling heat transfer coefficient and the critical heat flux method, with a graphite nano solution serving as the boiling working medium, analyzed was the influence of the graphite nano solution at various mass concentrations on the boiling heat transfer coefficient and critical heat flux density. The test results show that compared with deionized water, the graphite nano solution can enhance the boiling heat transfer coefficient. Under the test conditions, the heat transfer coefficient can maximally increase by 30%. When the concentration of graphite increases from 0.05 g/L to 2.5 g/L, the enhanced boiling heat transfer coefficient will first increase and then decrease. In the meantime, the nano solution will enhance the critical heat flux. With an increase of the concentration, the enhanced critical heat flux will first increase and then decrease. Among all the test conditions, the graphite nano solution at a concentration of 1 g/L will have a strongest ability in enhancing the boiling heat transfer and at such a time, the critical heat flux will be maximal. After the graphite nano solution had been boiled, the hydrophilicity of the heating surface will be enhanced and the static contact angle will become smaller, which is an important factor to enhance the critical heat flux. **Key words:** pool boiling, graphite, nano-fluid, heat transfer coefficient, critical heat flux

周向弯曲方向对 NACA65 翼型轴流叶轮叶顶间隙流动影响 = **Influence of the Bending Along the Circumferential Direction on the Flow in the Blade Tip Clearance in an Axial Flow Impeller Adopting the NACA65 Airfoil** [刊 汉]/YAN Pei-di, JIN Guang-yuan, CUI Zheng-wei (College of Mechanical Engineering, Jiangnan University, Wuxi, China, Post Code: 214122) // Journal of Engineering for Thermal Energy & Power. - 2016, 31(11). - 19 ~ 25

A straight impeller equipped with the NACA65-810 airfoil and impellers installed with blades forward and backwards bent respectively along the circumferential direction were designed by using a three-dimensional aerodynamic design method and a CFD (computational fluid dynamics) software was adopted to simulate their aerodynamic performance and analyze the spacial development of their leakage flows and vortexes in the three blade tip clearances beyond the impeller as well as the distribution of the static pressure losses and entropy in the blade tip clearances. It has been found that after the straight impeller had been forward bent along the circumferential direction, the entrainment ability of the leakage flow in the blade tip clearance will become weak and the initial location of the leakage vortexes will shift to a location away from the leading edge of the blades with the height of the center of the leakage vortex along the radial direction being kept unchanged, thus weakening the interference of the blade tip leakage vortex to the main stream. After the straight impeller had been backwards bent along the circumferential direction, the entrainment ability of the leakage flow in the blade tip clearance will become strong and the initial location of the leakage vortexes will shift to a location close to the leading edge of the blades with the height of the center of the leakage vortex along the radial direction away from the leading edge of the blade being notably lowered, thus expanding the dispersion range of the vortex core at the downstream, strengthening the interference of the blade tip leakage vortex with the main stream and unfavorable to lowering the blade tip leakage losses. **Key words:** NACA65 airfoil, bending along the circumferential direction, blade tip clearance, leakage flow, numerical analysis

三轴燃气轮机发电机组突变负载控制策略研究 = **Study of the Strategies for Controlling the Abruptly Changed Load of a Three-shaft Gas Turbine Power Generator Unit** [刊, 汉] / ZHANG Ya-dong, JIANG Li-yun, SONG Shao-hua, OU Yong-gang (Shenyang Engine Design Research Institute, China Aviation Industry Group Corporation, Shenyang, China, Post Code: 110015) // Journal of Engineering for Thermal Energy & Power. - 2016, 31(11). - 26 ~ 31

On the basis of the experiment and simulation of an integral machine, studied were the strategies for controlling the abruptly changed load of a three shaft gas turbine power generator unit. The test results show that the improved power forward feed + gas turbine rotating speed cascade PID closed cycle control version features a quick response, strong anti-interference ability and good self adaptability, thus capable of meeting the needs for transient power generation. In the case of an abrupt increase of a 40% load, the drop in the rotating speed of the power turbine will not be higher than 4% and the recovery time duration will not exceed 2 s. The simulation results show that in the case of load rejection, to open in advance the bleeding valve at the outlet of the low pressure air compressor to bleed air not only can improve the work allowance but also can contain the growth of the rotating speed of the power turbine. When the air quantity bled arrives at 25% of the rated air flow rate, the overshoot of the rotating speed of the power turbine will decline by 3% and the recovery time duration will shorten by 10 s compared with those when no air is bled. **Key words:** abruptly changed load, control strategy, cascade, forward feed, experiment and simulation